Transport regimes in surface disordered graphene sheets

E. Louis,[1] J. A. Vergés,[2] F. Guinea,[2] and G. Chiappe[1,3]
[1]*Departamento de Física Aplicada, Unidad Asociada del Consejo Superior de Investigaciones Científicas and Instituto Universitario de Materiales, Universidad de Alicante, San Vicente del Raspeig, Alicante 03690, Spain*
[2]*Departamento de Teoría de la Materia Condensada, Instituto de Ciencias de Materiales de Madrid (CSIC), Cantoblanco, Madrid 28049, Spain*
[3]*Departamento de Física J. J. Giambiagi, Facultad de Ciencias Exactas, Universidad de Buenos Aires, Ciudad Universitaria, 1428 Buenos Aires, Argentina*
(Received 7 February 2007; published 28 February 2007)

The conductance G of graphene stripes (of width W and length L) with surface disorder and near the Dirac point is investigated numerically. Incoherent metallic leads are attached to the sample ends across its width. In samples of $W/L \geqslant 1$, the system behaves diffusively with $G \to (2/\pi)(W/L) \times 2e^2/h$, for $L \to \infty$, as found in the clean limit, although with a sharply reduced shape dependence. The conductance in elongated samples, $L \gg W$, decays exponentially with L, indicating localization. A similar behavior is found in clean elongated systems due to the existence of minigaps near the Dirac point. Average decay lengths are *larger* in the presence of disorder. A magnetic field does not appreciably change the conductance unless the flux per unit cell is significant. The distribution of conductances is almost flat between lower and upper cutoffs. Away from the Dirac point, we find the standard ballistic behavior characteristic of systems with rough edges.

DOI: 10.1103/PhysRevB.75.085440 PACS number(s): 73.63.Fg, 71.15.Mb, 71.70.−d, 72.80.Ng

I. INTRODUCTION

The electronic transport in atomically thin graphene samples is a subject of great current interest.[1–7] The scaling with the sample dimensions[4] suggests a diffusive behavior, with a universal conductivity at the lowest carrier concentrations.[4,6] The limit of low concentration is difficult to analyze theoretically, as the Fermi wavelength becomes comparable to the separation between scatterers and even to the sample size. An analysis based on the Born approximation[8] leads to a universal conductivity at low temperatures $\sigma_t = (2/\pi)G_0$ ($G_0 = 2e^2/h$ being the conductance quantum), somewhat smaller than the one observed experimentally. The approximations involved in this approach, however, are expected to fail at the lowest concentrations. Explicit Landauer-type calculations show unusual scaling of the conductance for clean graphene systems at zero doping that is consistent with diffusive behavior[9] with a conductivity identical to that reported in Ref. 8 (for large samples much wider than longer). This pseudodiffusive behavior has also been found in SNS junctions[10] and graphene bilayers.[11] On the other hand, field theoretical arguments[12–14] suggest the existence of a localized regime in the limit of zero temperature and zero carrier concentration in the presence of disorder.

In this work, we numerically study the electronic transport in surface disordered graphene sheets both at finite dopings and in the limit of zero carrier concentration. As bulk disorder in graphene sheets seems to be rather low, we focus on the effects of rough edges, with disorder concentrated at the surface of the system. (See Fig. 1.) Our results at the Dirac point show that the pseudodiffusive regime identified in Ref. 9 persists in the presence of disorder with the same conductivity found in clean samples.[9] Some remarkable differences are worth commenting on. First, we note that the diffusive limit reported in Ref. 9 is obtained with a much weaker shape dependence. When plotting the conductance of samples of fixed width as a function of the sample length, an exponential decrease is obtained. In this way, the standard result for a quasi-one-dimensional (1D) system with any kind of disorder is recovered. In insulating graphene, however, this exponential decrease also applies to ordered samples. Actually, the presence of disorder slows down the exponential decay of those samples, showing a minigap at the Dirac point. In samples having a fixed length, the conductance is proportional to the sample width. These results can be rationalized in terms of transmission mediated by evanescent waves generated at the metallic leads. Away from the Dirac point, the conductance shows the ballistic behavior expected in two-dimensional (2D) systems with rough surfaces.

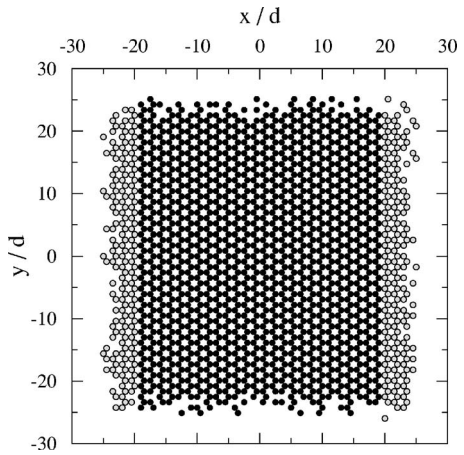

FIG. 1. Typical graphene sample of width W and length L used in the numerical calculations of the conductance presented in this work. The sample surface is disordered. Leads are attached to the lattice sites represented by gray circles.

II. METHODS: GRAPHENE SAMPLES AND CONDUCTANCE CALCULATIONS

We describe the valence and conduction bands of graphene by a tight-binding Hamiltonian with nearest-neighbor hoppings only,

$$\hat{H} = t\sum_{i,j} \hat{c}_i^{\dagger}\hat{c}_j + \text{H.c.}, \tag{1}$$

where sites i and j denote the nearest-neighbor nodes in the honeycomb lattice. Hereafter, the hopping integral t is taken as the unit of energy. The low-energy electronic spectrum, $|\epsilon_{\mathbf{k}}| \ll t$, can be approximated by the Dirac equation,

$$\epsilon_{\mathbf{k}} \approx \pm v_F|\mathbf{k}|, \tag{2}$$

where $v_F=(3td)/2$ and d is the distance between sites in the honeycomb lattice.

Surface-disordered samples of dimensions $L\times W$, $L(W)$ being the length (width) along (across) the transport direction, were produced by randomly removing an arbitrary percentage of sites at the sheet edges, typically 30% of the sites in the outer two atomic layers. Most calculations were done on samples produced by starting from ordered samples with "armchair" edges and having an axis of symmetry along the transport direction; such samples are insulating when ordered. In a few cases, we also considered samples with "metallic armchair" edges.[9] The leads were simulated by purely imaginary self-energies, independent of energy that were attached at the atoms of the sample ends. This choice is aimed at describing the probable incoherent nature of contacts.

The conductance was calculated by means of an efficient implementation of Kubo's formalism.[15] For a current propagating in the x direction, the static electrical conductance, spin degeneracy included, is given by

$$G = -2\left(\frac{e^2}{h}\right)\text{Tr}[(\hbar\hat{v}_x)\text{Im}\,\hat{G}(E)(\hbar\hat{v}_x)\text{Im}\hat{G}(E)], \tag{3}$$

where the velocity (current) operator $\hat{v}_x$ is related to the position operator $\hat{x}$ through the equation of motion $\hbar\hat{v}_x=[\hat{H},\hat{x}]$, $\hat{H}$ being the Hamiltonian. $\hat{G}(E)$ is the Green's function of the system with the leads already incorporated. All results include the spin degeneracy.

III. RESULTS

Figure 2 shows the conductance at the Dirac point versus $1/L$ for stripes without and with disorder, and $W=3L$, $5L$, and $11L$. The numerical results can be accurately fitted by quadratic curves such as $G(L/W)=(a+b/L+c/L^2)$, where $a\approx\sigma_t$ with an accuracy better than 1% for ordered samples with $W=3L$ and better than 0.1% in all other cases. It is worth noting that this limit is reached with incoherent contacts, as opposed to the coherent, momentum conserving contacts taken by other authors.[9] The effects of disorder are twofold: (i) A slight decrease of G not larger than 3% for the results shown in the figure and (ii) a significant reduction of the shape dependence of G [results for different W/L ratios almost collapse (see Fig. 2)]. These conclusions are further

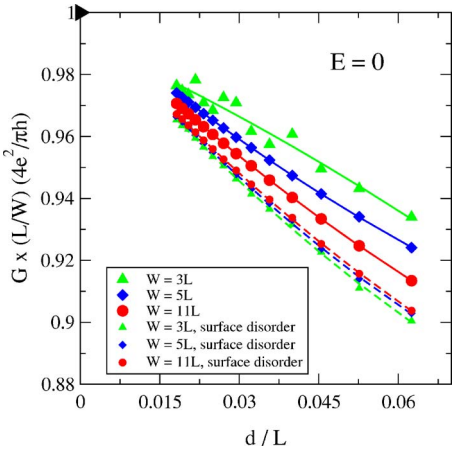

FIG. 2. (Color online) Scaling of the conductance obtained for ordered and surface disordered stripes of different width (W) over length (L) ratios as a function of d/L. All data converge to 1 (black triangle in the upper left corner of the figure) for $L\to\infty$ according to quadratic fits in powers of L^{-1} (continuous lines).

illustrated by the results for $G(L/W)$ in the upper panel of Fig. 3. Certainly, although fluctuations sharply increase as the ratio W/L decreases (as W/L increases, the conductance becomes increasingly dominated by metallic tails which have a low sensitivity to surface disorder), the results for $W=0.5L$, L, and $2L$ do approximately collapse around σ_t (actually, the average values are $0.94\sigma_t$, $0.97\sigma_t$, and $0.96\sigma_t$, respectively). Away from the Dirac point (see the results for $E=0.1t$ in the upper panel of Fig. 3), the conductance increases linearly with W. This is the expected ballistic behavior of a quantum billiard with either surface disorder or with an amount of defects proportional to L (a defect concentration decreasing as $1/L$).[16,17] We also note that fluctuations

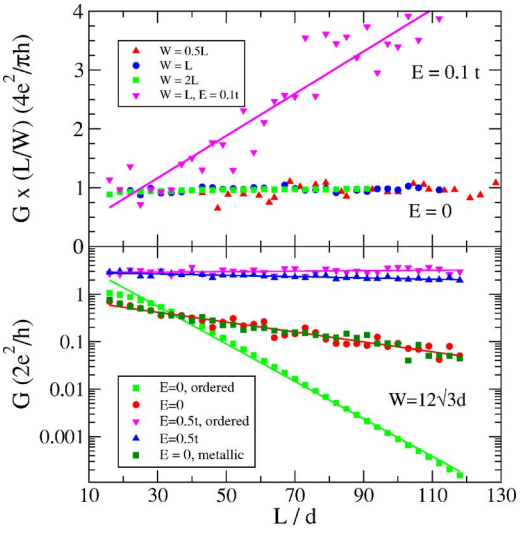

FIG. 3. (Color online) Top panel: scaling with length L of the conductance in samples with several fixed W/L ratios and surface disorder. Bottom panel: scaling with length of stripes of fixed width. The points labeled metallic correspond to a stripe with a subband crossing at $E=0$. All other samples have finite-size gaps near the band center.

away from the Dirac point are enhanced as a consequence of the effects that surface disorder has on graphene electronic states that control transport at those energies (as opposed to the metallic-tail controlled conductance at the Dirac point).

This pseudodiffusive regime of clean systems has been already analyzed in Ref. 9. In an ideal square system, the incoming channels can be characterized by the transverse momentum k_y. The electronic spectrum of a graphene stripe at finite transverse momentum shows a gap for $-v_F|k_y| \leqslant \epsilon \leqslant v_F|k_y|$. Hence, states with transverse momentum k_y decay away from the boundaries as $e^{-|k_y|x}$ and lead to a transmission $T_{k_y} \propto e^{-2|k_y|L}$. The number of channels scales as the width of the system W. In sufficiently large systems, the sum over channels can be replaced by an integral over k_y leading to a conductance which scales as $G \propto WL^{-1}$.

Results for the conductance versus L in samples of fixed width are depicted in the lower panel of Fig. 3. At the Dirac point, the conductance of samples decays exponentially with L at a pace which is the same for disordered samples built up from either insulating or metallic-ordered samples. On the other hand, the conductance in ordered samples either decreases exponentially in insulating samples (see also Fig. 3) or remains constant in metallic samples (not shown in the figure). Surface disorder eliminates the effects of the boundary conditions, as one could have easily guessed. On the other hand, the decay length is shorter in clean samples than in disordered samples, leading to an enhancement of the conductance in semiconducting disordered samples at $E=0$. This enhancement is probably related to the formation of resonances at $E=0$ near defects, whose existence has been well established at edges,[18,19] cracks,[20] vacancies,[21] and line defects transverse to the transport direction.[22] Away from the Dirac point, while the conductance in ordered samples remains constant, it decreases exponentially in surface disordered systems (see lower panel of Fig. 3), although with a localization length much longer than that found at $E=0$; this behavior is typical of two-dimensional billiards with surface disorder.

The scaling of the conductance with the width of a sheet of constant length is shown in Fig. 4. The results clearly indicate that the conductance increases linearly with the sample width with a slope that depends on the concentration of carriers (or the energy). This result is characteristic of both ballistic and diffusive behaviors in 2D and cannot therefore be used to discriminate the transport regime in this case. A remarkable feature of the results shown in Fig. 4 is the low dispersion at the Dirac point. This can be understood by noting that the increase in conductance is exclusively due to an increasing number of metallic tails through the bulk of the graphene sheet and is therefore weakly sensitive to surface disorder.

The conductance distribution $P(G)$ for samples of an approximate square shape at $E=0$ further illustrates the role of metallic tails. As shown in Fig. 5, $P(G)$ has well-defined lower and upper bounds, being almost constant within the range over which it is finite (actually it decreases slightly with G). Those bounds do depend on the ratio W/L. This distribution is rather odd, and its origin can be traced back to the metallic tails. In particular, a null probability at $G=0$ [at variance with what occurs in standard billiards with a single channel, (see Ref. 23)] is likely due to the fact that surface disorder cannot completely eliminate the contribution of the metallic tails.

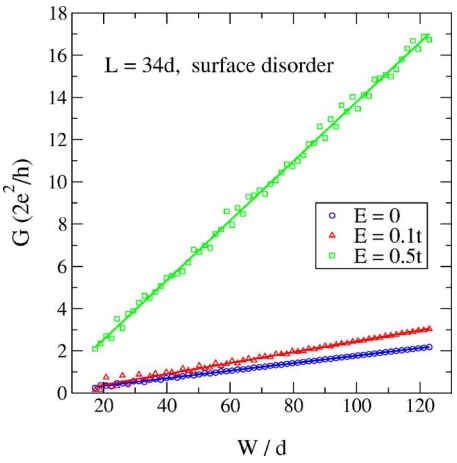

FIG. 4. (Color online) Conductance (in units of the conductance quantum) through surface disordered graphene samples of size $W \times 24d$ versus the sample width W.

A uniform magnetic field perpendicular to the sample surface is included in the tight-binding Hamiltonian [Eq. (1)] in the usual way, that is, calculating the total flux traversing any hexagonal plaquette and adding the corresponding phase to one of the links forming the hexagon. Some matrix elements of the operator become complex, but the calculation of electric currents through the sample remains identical. The conductance for $36d \times 40d$ and $34d \times 80d$ samples versus the magnetic-field intensity is plotted in Fig. 6. The results correspond to the average over 12 disorder realizations. Individual results for any of the 12 realizations are only shown for the square sample, since in the elongated sample, fluctuations are much weaker (see above). The relation between total flux and magnetic field is explained in the figure cap-

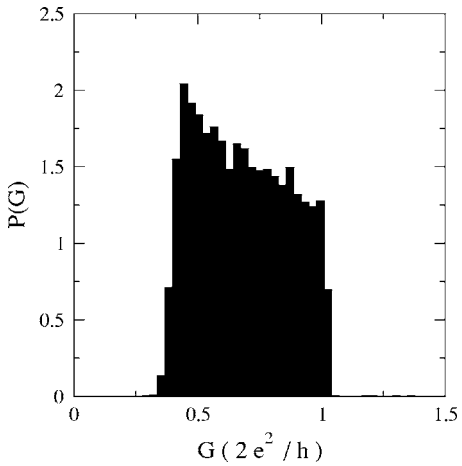

FIG. 5. Conductance distribution $P(G)$ obtained at $E=0$ for a set of 10 000 graphene randomly generated samples with size of $24d \times 24d$ with surface disorder. Surface vacancies (around 30%) were introduced in two atomic layers around the sample surface. Incoherent metallic contacts are attached at opposite sides of the sample (see text).

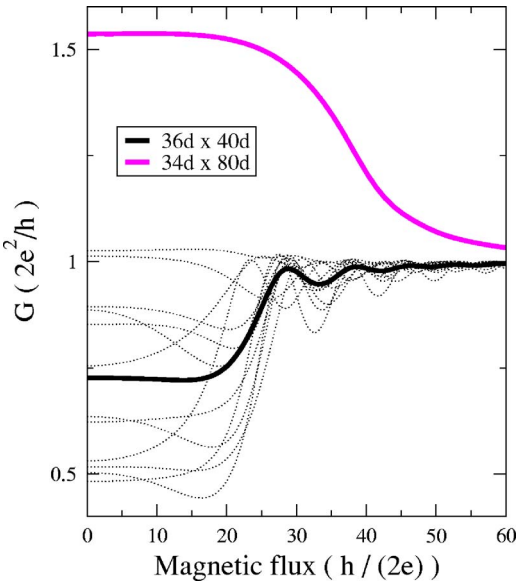

FIG. 6. (Color online) Conductance at the Dirac point as a function of the total magnetic flux through the graphene lattice in $36d \times 40d$ and $34d \times 80d$ samples with disorder at the edges. Thick continuous lines depict averages over 12 realizations of disorder, while dotted lines correspond to the 12 realizations of the square sample. A magnetic field of 1 T corresponds approximately to 0.019 ($36d \times 40d$ samples) and 0.038 ($34d \times 80d$ samples) flux units through the sample.

tion. In both samples, the conductance remains constant up to fields $\approx$1600 T (around 0.05 flux quanta per unit cell), becoming approximately one quantum unit thereafter. This indicates that no weak localization effects[24] are expected to show up. In addition, once the conductance quantum is attained, the conductance in the almost square sample shows no dependence on disorder realization. The magnetoconductance in this limit is dominated by lattice effects, as the flux per unit cell becomes significant; this also explains the sharp reduction of the fluctuations that characterize the conductance at zero field. We note, however, that this regime cannot be reached for fields attainable in the laboratory. Our findings are consistent with semianalytical calculations using a continuum model in the clean limit.[25] They lead to an alternative explanation of the observed absence of weak localization effects[26–28] at very low dopings.

IV. CONCLUDING REMARKS

In conclusion, we have presented a detailed numerical calculation of the conductance of disordered graphene at the neutrality point, where quasiclassical arguments cannot be applied. Our results show that in samples of comparable width and length, the system behaves diffusively, the transport being dominated by evanescent waves as in the clean case.[9–11,29] The conductivity per unit area which can be defined in this regime is close to $4e^2/(\pi\hbar)$, as in clean samples, although the disorder at the edges considered here significantly reduces the shape dependence. Localization effects, while observed, only play a role in quasidimensional samples, $L \gg W$. We have also shown that magnetic fields of strengths attainable in laboratories do not lead to appreciable changes in the conductance unlike the expected behavior in truly diffusive or localized systems.

ACKNOWLEDGMENTS

Financial support by the Spanish MCYT (Grant Nos. FIS200402356, MAT2005-07369-C03, FIS2005-05478-C02-01, and NAN2004-09183-C10-08), the Generalitat Valenciana (Grant Nos. GRUPOS03/092 and GV05/152), the Universidad de Buenos Aires (Grant No. UBACYT x115), and the Argentinian CONICET is gratefully acknowledged. G.C. is thankful to the Spanish MEC for a Ramón y Cajal grant. F.G. acknowledges funding from the European Union Contract No. 12881 (NEST) and the Comunidad de Madrid, through the program CITECNOMIK, CM2006-S-0505-ESP-0337.

[1] K. S. Novoselov, A. K. Geim, S. V. Morozov, D. Jiang, Y. Zhang, S. V. Dubonos, I. V. Gregorieva, and A. A. Firsov, Science **306**, 666 (2004).
[2] C. Berger, Z. M. Song, T. B. Li, X. B. Li, A. Y. Ogbazghi, R. Feng, Z. T. Dai, A. N. Marchenkov, E. H. Conrad, P. N. First *et al.*, J. Phys. Chem. B **108**, 19912 (2004).
[3] J. S. Bunch, Y. Yaish, M. Brink, K. Bolotin, and P. L. McEuen, Nano Lett. **5**, 2887 (2005).
[4] K. S. Novoselov, A. K. Geim, S. V. Morozov, D. Jiang, M. I. Katsnelson, I. V. Grigorieva, S. V. Dubonos, and A. A. Firsov, Nature (London) **438**, 197 (2005).
[5] K. S. Novoselov, D. Jiang, F. Schedin, T. J. Booth, V. V. Khotkevich, S. V. Morozov, and A. K. Geim, Proc. Natl. Acad. Sci. U.S.A. **102**, 10451 (2005b).
[6] Y. Zhang, Y.-W. Tan, H. L. Stormer, and P. Kim, Nature (London) **438**, 201 (2005).
[7] S. V. Morozov, K. S. Novoselov, F. Schedin, D. Jiang, A. A. Firsov, and A. K. Geim, Phys. Rev. B **72**, 201401(R) (2005).
[8] N. M. R. Peres, F. Guinea, and A. H. Castro Neto, Phys. Rev. B **73**, 125411 (2006).
[9] J. Tworzydlo, B. Trauzettel, M. Titov, A. Rycerz, and C. W. J. Beenakker, Phys. Rev. Lett. **96**, 246802 (2006).
[10] M. Titov and C. W. J. Beenakker, Phys. Rev. B **74**, 041401(R) (2006).
[11] I. Snyman and C. W. J. Beenakker, Phys. Rev. B, **75**, 045322 (2007).
[12] I. L. Aleiner and K. B. Efetov, Phys. Rev. B **74**, 075102 (2006).
[13] A. Altland, Phys. Rev. B **65**, 104525 (2002).
[14] P. M. Ostrovsky, I. V. Gornyi, and A. D. Mirlin, Phys. Rev. B **74**, 235443 (2006).
[15] J. A. Vergés, Comput. Phys. Commun. **118**, 71 (1999).
[16] E. Cuevas, E. Louis, and J. A. Vergés, Phys. Rev. Lett. **77**, 1970 (1996).
[17] J. A. Vergés and E. Louis, Phys. Rev. E **59**, R3803 (1999).

[18] K. Wakabayashi and M. Sigrist, Phys. Rev. Lett. **84**, 3390 (2000).
[19] K. Wakabayashi, Phys. Rev. B **64**, 125428 (2001).
[20] M. A. H. Vozmediano, M. P. L ópez-Sancho, T. Stauber, and F. Guinea, Phys. Rev. B **72**, 155121 (2005).
[21] V. M. Pereira, F. Guinea, J. M. B. LopesdosSantos, N. M. R. Peres, and A. H. CastroNeto, Phys. Rev. Lett. **96**, 036801 (2006).
[22] M. Titov, cond-mat/0611029 (unpublished).
[23] H. U. Baranger and P. A. Mello, Phys. Rev. B **54**, R14297 (1996).
[24] E. Louis and J. A. Vergés, Phys. Rev. B **63**, 115310 (2001).
[25] E. Prada, P. San-José, B. Wunsch, and F. Guinea, cond-mat/0611189 (unpublished).
[26] S. V. Morozov, K. S. Novoselov, M. I. Katsnelson, F. Schedin, L. A. Ponomarenko, D. Jiang, and A. K. Geim, Phys. Rev. Lett. **97**, 016801 (2006).
[27] A. F. Morpurgo and F. Guinea, Phys. Rev. Lett. **97**, 196804 (2006).
[28] E. McCann, K. Kechedzhi, V. I. Fal'ko, H. Suzuura, T. Ando, and B. L. Altshuler, Phys. Rev. Lett. **97**, 146805 (2006).
[29] C. W. J. Beenakker, Phys. Rev. Lett. **97**, 067007 (2006).